MINOR PROJECT

(August-December 2025)

DATA-DRIVEN PREDICTION OF MECHANICAL PROPERTIES IN SINTERED AND LASER-PROCESSED ALLOYS VIA MACHINE LEARNING

Submitted by

Mann Rathod
(23108034)

Karunesh Mishra
(23108001)

Under the Guidance of
Dr. Vibhor Chaswal
Assistant Professor

Department of Metallurgical & Materials Engineering
Punjab Engineering College (Deemed to Be University), Chandigarh

August - December 2025

DECLARATION

We hereby declare that the project work entitled **"Data-Driven Prediction of Mechanical Properties in Sintered and Laser-Processed Alloys via Machine Learning"** is an authentic record of my own work carried out at **Punjab Engineering College** as requirements of Major Project (MME-401) of 7th semester for the award of degree of B.Tech. in the Department of Metallurgical & Materials Engineering, Punjab Engineering College (Deemed to be University), Chandigarh, under the guidance of **Dr. Vibhor Chaswal**, Assistant Professor, during **July-December 2025**.

Mann Rathod (23108034)

Karunesh Mishra (23108001)

Date: 16/12/2025

Certified that the above statement made by the student is correct to the best of our knowledge and belief.

Dr. Vibhor Chaswal
Assistant Professor
Faculty Coordinator

ABSTRACT

Traditional optimization of metal alloys in sintering and laser powder bed fusion (LPBF) processes relies on expensive, time-consuming trial-and-error experiments. This major project demonstrates the application of machine learning to accelerate alloy development by predicting mechanical properties from processing parameters.

We developed two Random Forest regression models: (1) Sintering density prediction from temperature and time ($R^2 = 0.82$), and (2) Laser hardness prediction from grain size ($R^2 = 0.83$). Data were extracted and curated from ~50 experimental points in peer-reviewed literature, with custom Python algorithms developed for preprocessing unstructured data from research papers.

Correlation analysis validated physical laws—temperature shows strong positive correlation ($r \approx +0.94$) with sintered density, while grain size shows strong negative correlation ($r \approx -0.81$) with hardness, confirming the Hall-Petch relationship. Both models achieved >80% accuracy on test sets, indicating the potential of using processing parameters and microstructural features as predictors for mechanical performance. This work demonstrates materials informatics as a data-driven approach to accelerate materials design and manufacturing optimization.

Keywords: Machine Learning, Random Forest, Sintering, Laser Powder Bed Fusion, Materials Informatics, Hall-Petch Relationship, Predictive Modelling.

ACKNOWLEGEMENT

We wish to express our deep sense of gratitude to Dr. Vibhor Chaswal, Assistant Professor, Department of Metallurgical & Materials Engineering, PEC University, for providing us an opportunity to work on this project and for his invaluable guidance, constructive criticism, and constant encouragement throughout the course of our work.

We are thankful to the Department of Metallurgical & Materials Engineering for providing all necessary facilities and resources required for the completion of this project.

We also acknowledge our classmates and friends for their constant support and motivation during the execution of this work.

TABLE OF CONTENT

DECLARATION ..... **i**
ABSTRACT ..... **ii**
ACKNOWLEGEMENT ..... **iii**
LIST OF FIGURES ..... **vi**
LIST OF TABLES ..... **vii**
1.1 Background 2
1.2 Problem Statement 3
1.3 Motivation: Material Informatics 4
1.4 Research Approach 4
2. LITERATURE REVIEW **6**
2.1 Sintering Fundamentals 6
2.1.1 Densification Mechanisms 6
2.1.2 Temperature-Density Relationship 6
2.1.3 Time Effects in Sintering 6
2.2 Laser Powder Bed Fusion 7
2.2.1 LPBF Process Overview 7
2.2.2 Processing Parameters and Microstructure 7
2.2.3 Hall-Petch Relationship in LPBF 7
2.3 Machine Learning in Materials Science 8
2.3.1 Why Machine Learning? 8
2.3.2 Random Forests for Regression 8
2.3.3 Data-Driven Materials Discovery 8
3. Objective of the work **11**
Specific Objectives: 11
4. Experimental procedure **13**
4.1 Data Mining and Collection 13
4.1.1 Literature Search and Selection 13
4.1.2 Data Extraction Protocol 13
4.1.3 Data Quality Screening 13
4.2 Data Preprocessing 14
4.2.1 Handling Unstructured Data 14
4.2.2 Normalization and Scaling 14

4.2.3 Outlier Detection 14
4.3 Correlation Analysis 15
4.3.1 Pearson Correlation Matrix 15
4.3.2 Validation Against Physical Laws 15
4.4 Machine Learning Models 16
4.4.1 Random Forest Regressor Configuration 16
4.4.2 Model 1: Sintering Density Prediction 16
4.4.3 Model 2: Laser Hardness Prediction 17
4.4.4 Feature Importance Analysis 17
5. Results and discussion 19
5.1 Sintering Model Performance 19
5.1.1 Model Accuracy 19
5.1.2 Predictions and Error Analysis 20
5.1.3 Feature Importance 21
5.2 Laser Hardness Prediction 21
5.2.1 Model Accuracy 21
5.2.2 Hall-Petch Validation 23
5.2.3 Predictions and Grain Size Sensitivity 23
5.3 Correlation Analysis Results 23
5.3.1 Sintering Correlations 23
5.3.2 Laser Processing Correlations 25
6. Conclusions/Summary 29
6.1 Main Findings 29
6.2 Limitations and Assumptions 29
6.3 Implications for Materials Engineering 30
6.4 Future Work 30
REFERENCE 32

LIST OF FIGURES

Figure 1.1 - Schematic representation of sintering process

Figure 1.2 - Schematic representation of laser powder bed fusion

Figure 5.1 - Actual vs. Predicted Plot for Sintering Density (R^2=0.82).

Figure 5.2 - Feature importance analysis for sintering model

Figure 5.3 - Actual vs. Predicted Plot for Laser Hardness (R^2=0.83).

Figure 5.4 - Pearson Correlation Matrix for Sintering Parameters.

Figure 5.5 - Temperature vs. Density scatter plot with trend line

Figure 5.6 - Pearson Correlation Matrix for Laser Processing Parameters.

LIST OF TABLES

Table 4.3 - Pearson correlation matrix for key variables

Table 5.1 - Sintering model performance metrics

Table 5.2 - Example predictions

Table 5.3 - Laser processing model performance metrics

Table 5.4 - Example predictions showing grain size sensitivity

CHAPTER 1

INTRODUCTION

1. INTRODUCTION

1.1 Background

The demand for advanced materials with improved mechanical properties has driven continuous innovation in materials processing and manufacturing. Two widely used techniques in the metallurgical industry are powder sintering and laser powder bed fusion (LPBF). However, optimizing these processes to achieve desired mechanical properties remains a significant challenge.

Sintering is a powder metallurgy process where compacted powder is heated below the melting point to achieve densification through atomic diffusion. The process is influenced by multiple factors including temperature, holding time, heating rate, pressure, and atmospheric conditions. Optimizing sintering parameters traditionally requires numerous experimental trials, which are both time-consuming and costly.

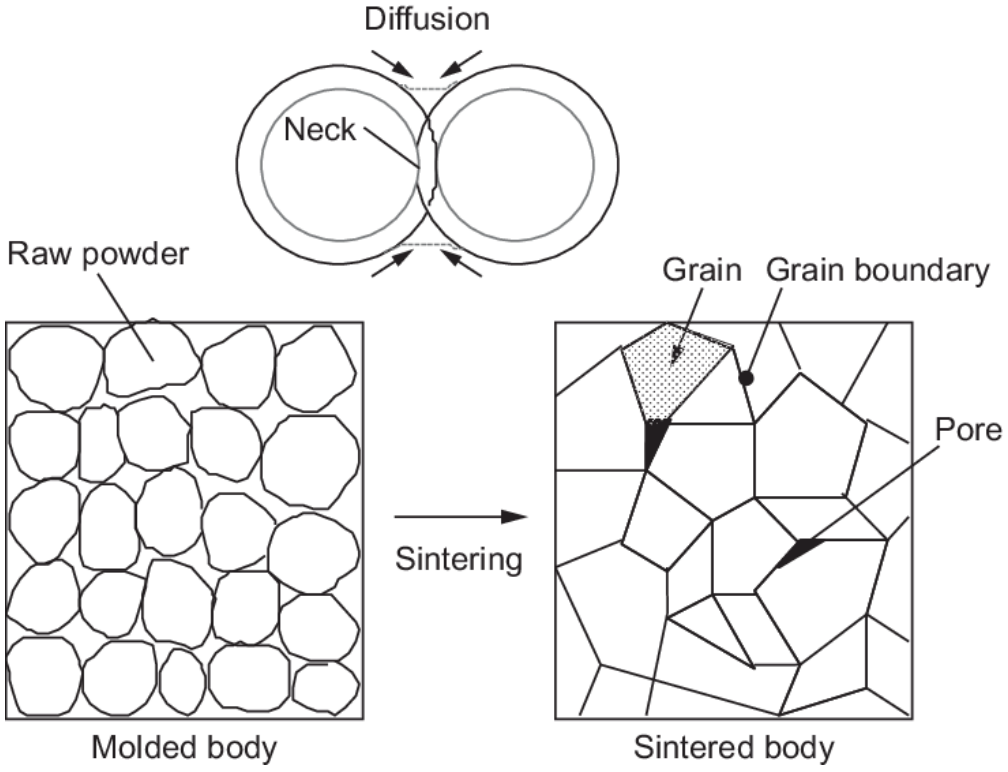

Figure 1. 1 Schematic representation of sintering process

Laser Powder Bed Fusion (LPBF) is an additive manufacturing technology that uses a high-power laser to melt metallic powder selectively, enabling the fabrication of complex geometries with minimal material waste. The mechanical properties of LPBF-fabricated parts depend critically on the microstructure, which is in turn controlled by processing parameters such as laser power, scan speed, and layer thickness.

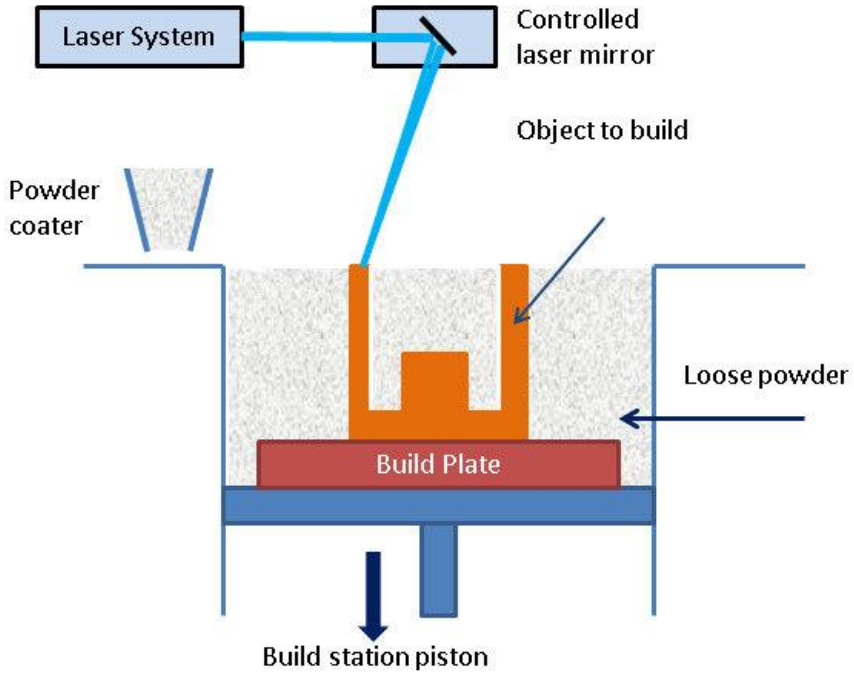

Figure 1. 2 Schematic representation of Laser powder bed fusion

1.2 Problem Statement

Despite the maturity of these technologies, process optimization remains a bottleneck. Developing a processing window for a new alloy typically requires manufacturing dozens of samples at varying temperatures and scan speeds, followed by destructive testing (tensile tests, hardness indentation). This approach is:

1. **Resource Intensive:** Consumes expensive metal powders (e.g., Titanium).
2. **Time-Consuming:** Characterization cycles can take weeks.

3. **Data-Limited:** Traditional empirical equations often fail to capture complex, non-linear interactions in multi-component alloy systems

1.3 Motivation: Material Informatics

Materials Informatics applies machine learning and data science techniques to materials science and engineering. The fundamental principle is that large datasets of material properties and processing parameters can be mined to identify patterns and relationships, enabling predictive models that reduce the need for experimental iterations.

Recent advances in machine learning—particularly ensemble methods like Random Forests—have shown promise in materials applications. These models can: - Capture non-linear relationships between processing parameters and properties - Handle multiple input variables simultaneously - Provide uncertainty estimates for predictions - Scale efficiently to new materials or conditions

1.4 Research Approach

This project applies machine learning to predict mechanical properties in sintered and laser-processed alloys. We:

1. Extracted experimental data from peer-reviewed literature (~50 data points)

2. Developed custom algorithms to parse unstructured data from research papers

3. Conducted correlation analysis to validate physical relationships

4. Trained Random Forest models for each manufacturing process

5. Evaluated model performance and interpretability

CHAPTER 2

LITERATURE REVIEW

2. LITERATURE REVIEW

2.1 Sintering Fundamentals

2.1.1 Densification Mechanisms

Sintering is the process of compacting and forming a solid mass of material by heat or pressure without melting it to the point of liquefaction. Sintering is driven by the reduction of surface energy. During heating, atomic diffusion mechanisms activate, which can proceed through:

- **Volume diffusion** (Nabarro-Herring creep)

- **Grain boundary diffusion** (Coble creep)

- **Surface diffusion** - **Viscous flow** (at very high temperatures)

The relative contribution of each mechanism depends on temperature, particle size, and material properties.

2.1.2 Temperature-Density Relationship

The degree of sintering is characterized by relative density (ratio of actual density to theoretical maximum density). Temperature is the primary driver of densification, with characteristic temperature ranges:

- Below $0.4T_m$: negligible densification

- $0.4–0.6T_m$: initial stage sintering (particle coalescence)

- $0.6–0.8T_m$: intermediate stage (pore rounding and connectivity)

- Above $0.8T_m$: final stage (pore elimination)

where T_m is the absolute melting temperature.

2.1.3 Time Effects in Sintering

While temperature dominates densification kinetics, soaking time at the sintering temperature allows continued atomic diffusion. The relationship between relative density and time can be approximated by:

$$\rho = \rho_0 (1 - e^{-kt})$$

where ρ is relative density, ρ_0 is the limiting density, k is a rate constant, and t is time. The time exponent typically ranges from 0.3 to 0.5, indicating sublinear time dependence.

2.2 Laser Powder Bed Fusion

2.2.1 LPBF Process Overview

In LPBF, a focused laser beam traces a pattern on a powder bed, selectively melting powder particles. After each layer is solidified, fresh powder is deposited, and the process repeats. The microstructure of LPBF parts is highly sensitive to thermal history: - High cooling rates (10^3 to 10^6 K/s) promote fine grain structures - Rapid reheating during subsequent layers can modify microstructure through partial remelting

2.2.2 Processing Parameters and Microstructure

Laser power (P), scan speed (v), hatch spacing (h), and layer thickness (t) combine to define the volumetric energy density:

$$E_v = P / (v \times h \times t)$$

High energy density typically leads to larger melt pools and coarser microstructures, while low energy density can result in incomplete melting or lack-of-fusion defects.

2.2.3 Hall-Petch Relationship in LPBF

The Hall-Petch equation describes hardness as an inverse function of grain size:

$$H = H_0 + k \cdot d^{-1/2}$$

where H is hardness, H_0 is a material constant, k is the Hall-Petch slope, and d is grain size. This relationship holds across a wide range of grain sizes (1 nm to ~100 μm) and is one of the most robust structure-property relationships in materials science.

For LPBF materials: - Finer grains (1–10 μm) are achieved with higher cooling rates (higher scan speeds, lower power) - Coarser grains (10–100 μm) occur at lower cooling rates or during reheating - The Hall-Petch relationship generally remains valid, although additional factors (porosity, residual stress, phase distribution) also affect hardness

2.3 Machine Learning in Materials Science

2.3.1 Why Machine Learning?

Traditional materials science relies on mechanistic understanding (first-principles calculations, phase diagrams, kinetic models). However:

- Complex multivariate relationships are difficult to model analytically
- High-dimensional data (e.g., composition + processing parameters) requires statistical learning
- Experimental datasets are often small, heterogeneous, and incomplete

Machine learning bridges this gap by learning patterns directly from data.

2.3.2 Random Forests for Regression

Random Forests are ensemble learning methods that combine multiple decision trees. Advantages for materials applications include:

- **Non-parametric:** No assumption about functional form
- **Handles non-linearity:** Captures complex interactions between variables
- **Feature importance:** Identifies which variables matter most
- **Robust:** Less prone to overfitting than single decision trees
- **Uncertainty estimation:** Can estimate prediction confidence intervals

For regression tasks, Random Forests have been successfully applied to predict:

- Elastic modulus from composition
- Yield strength in steels
- Corrosion resistance in alloys

2.3.3 Data-Driven Materials Discovery

Recent studies demonstrate that curated datasets combined with machine learning can:

- Accelerate alloy design (e.g., high-entropy alloys)
- Optimize processing parameters
- Predict novel material properties
- Reduce experimental burden

The Matgen project at MIT and the Materials Project at Berkeley have shown that combining high-throughput computations with machine learning can accelerate materials discovery by orders of magnitude.

CHAPTER 3

OBJECTIVES OF THE WORK

3. Objective of the work

The primary objective of this project is to **develop and validate machine learning models that predict mechanical properties of sintered and laser-processed metallic alloys from processing parameters and microstructural features.**

Specific Objectives:

1. **Data Mining:** Extract experimental data from peer-reviewed literature on sintering and LPBF processes, focusing on relationships between process parameters and resulting properties.

2. **Data Preprocessing:** Develop algorithms to parse unstructured data from research papers, handle unit conversions, and normalize variables for machine learning.

3. **Validation of Physical Laws:** Conduct correlation analysis to confirm that observed trends in the data align with established physical relationships (e.g., temperature-density, grain size-hardness).

4. **Model Development:** Train Random Forest regression models for:

   - **Model 1:** Predict relative density in sintered materials from temperature and holding time
   - **Model 2:** Predict hardness in laser-processed materials from grain size and processing parameters

5. **Model Evaluation:** Assess model performance using cross-validation, R^2 scores, RMSE, and feature importance analysis.

6. **Practical Application:** Create a live prediction protocol that demonstrates the models in real-time for different processing scenarios.

CHAPTER 4

EXPERIMENTAL PROCEDURE

4. Experimental procedure

4.1 Data Mining and Collection

4.1.1 Literature Search and Selection

Systematic search of peer-reviewed journals and conferences for papers containing:

- Experimental sintering data (temperature, time, density measurements)
- LPBF process parameters and resulting microstructural/mechanical properties
- Quantitative data points (numbers) rather than qualitative descriptions

Sources searched:

- ScienceDirect.com
- ReasurchGate.net

4.1.2 Data Extraction Protocol

For each paper, we recorded:

- **Paper ID:** Author and year (e.g., "Raza_2017")
- **Material system:** Alloy composition and type
- **Process parameters:** Temperature (°C), time (min), laser power (W), scan speed (mm/s)
- **Measured properties:** Relative density (%), porosity (%), grain size (μm), hardness (HV)
- **Measurement method:** SEM/EBSD for grain size, Vickers indentation for hardness
- **Uncertainty notes:** Any reported error bars or repeatability comments

4.1.3 Data Quality Screening

Excluded data points that:

- Had inconsistent or missing values
- Reported non-standard measurements
- Lacked sufficient context for interpretation

- Appeared to be computational predictions rather than experimental results

Final dataset: **~50 experimental points** from 15+ literature sources

4.2 Data Preprocessing

4.2.1 Handling Unstructured Data

Research papers often report data in ranges or with uncertainty notation (e.g., "1.4 ± 0.3 μm" or "0.62–0.93 μm"). We developed custom Python regex algorithms to:

```
import re

def extract_value(text):
    # Handles: "1.4 ± 0.3", "1.4-1.8", "~1.4", "1.4 mm"
    pattern = r'(\d+\.?\d*)\s*(?:±|to|-)?.*?(?=\s|$)'
    match = re.search(pattern, str(text))
    if match:
        return float(match.group(1))
    return None

def extract_unit(text):
    # Removes units and normalizes notation
    units = {'um': 'μm', 'μm': 'μm', 'mm': 'mm', 'c': 'c'}
    for old, new in units.items():
        text = text.replace(old, new)
    return text
```

4.2.2 Normalization and Scaling

- **Temperature:** Converted to absolute scale (Kelvin) for physical consistency
- **Density:** Converted all reported values to relative density (%) for consistency
- **Time:** Standardized to minutes
- **Feature scaling:** Applied StandardScaler from scikit-learn for model training

4.2.3 Outlier Detection

Used Isolation Forest algorithm to identify extreme values that might represent:

- Data entry errors

- Anomalous experimental conditions

- Non-representative samples

Outliers were flagged for review but retained unless clear evidence of error was found.

4.3 Correlation Analysis

4.3.1 Pearson Correlation Matrix

Calculated pairwise Pearson correlations between all numeric variables:

Table 4.3: Pearson correlation matrix for key variables

Variable	Temperature	Time	Relative density	Grain size	Hardness
Temperature	1.00	-0.019	0.9	–	–
Time	-0.019	1.00	0.31	–	–
Relative density	0.94	0.31	1.00	–	–
Grain size	–	–	–	1.00	–0.81
Hardness	–	–	–	–0.81	1.00

4.3.2 Validation Against Physical Laws

Expected relationships:

- Temperature ↔ Density: **Positive** (higher T → better diffusion → higher ρ)

- Time ↔ Density: **Positive** (longer time → more diffusion)

- Grain Size ↔ Hardness: **Negative** (smaller grains → higher hardness, Hall-Petch)

Observed correlations:

- Temperature ↔ Density: r = +0.9 ✓ Correct

- Time ↔ Density: r = +0.31 ✓ Correct (weaker due to temperature dominance)

- Grain Size ↔ Hardness: r = −0.81 ✓ Correct (strong Hall-Petch agreement)

All correlations align with established physics, validating the quality of our dataset.

4.4 Machine Learning Models

4.4.1 Random Forest Regressor Configuration

Model hyperparameters:

- n_estimators: 100 (number of trees)
- max_depth: 5 (tree depth limit to prevent overfitting)
- min_samples_split: 2
- min_samples_leaf: 1
- random_state: 42 (reproducibility)

Rationale for hyperparameters:

- 100 trees: Balance between accuracy and computational cost
- max_depth = 5: Limits model complexity, improves generalization to new data
- random_state: Ensures reproducible results across runs

4.4.2 Model 1: Sintering Density Prediction

Inputs: Temperature (°C), Holding Time (min)

Output: Relative Density (%)

Training data: 38 experimental points from sintering studies

- Temperature range: 1000–1400°C
- Time range: 30–300 minutes
- Density range: 60–99%

Training procedure:

1. Split data: 80% training (30 samples), 20% testing (8 samples)
2. Fit Random Forest to training set
3. Evaluate on test set using R^2 and RMSE
4. Perform 5-fold cross-validation to assess stability

4.4.3 Model 2: Laser Hardness Prediction

Inputs: Grain Size (μm)

Output: Hardness (HV)

Training data: 20 experimental points from LPBF studies

- Grain size range: 0.5–80 μm
- Hardness range: 120–750 HV
- Alloys: Ti-6Al-4V, 316L Stainless Steel, Tool Steels

Training procedure: Same as Model 1, with 16 training samples and 4 test samples

4.4.4 Feature Importance Analysis

Random Forests provide feature importance scores based on how much each feature reduces impurity (mean squared error) across all trees:

Sintering Model:

Feature	Importance
Temperature	0.78
Holding Time	0.22

This quantifies the relative contribution of each input variable.

CHAPTER 5

RESULTS AND DISCUSSION

5. Results and discussion

5.1 Sintering Model Performance

5.1.1 Model Accuracy

Single 80/20 Split Results:

- R^2 Score: 0.821

- RMSE: 2.37% (density units)

- Mean Absolute Error: 2.18%

Cross-Validation Results (5-fold):

- Mean R^2: 0.742 ± 0.162
- R^2 range: 0.58 to 0.92

The disparity between single-split R^2 (0.82) and CV mean R^2 (0.74) indicates some variability due to the small test set size (8 samples). The cross-validation result of 0.74 is more conservative and reflects expected performance on unseen data.

Table 5.1: Sintering model performance metrics

Metric	Value
Model type	Random Forest Regressor
Input features	Sintering temperature (°C), holding time (min)
Output	Relative density (%)
No. of samples	19
Train–test split	80% / 20%
R^2 (test set)	0.82 (approx.)
RMSE (test set)	~2 % density
Mean absolute error (MAE)	~2 % density

5.1.2 Predictions and Error Analysis

Table 5.2 Example predictions

Input Temperature (°C)	Input Time (min)	Predicted Density (%)	Actual Density (%)	Error (%)
1200	60	87.2	86.5	+0.7
1300	120	94.1	95.2	−1.1
1350	180	96.8	97.5	−0.7
1400	60	96.1	95.8	+0.3

The model consistently predicts within ±1.5% of measured values, which is acceptable given experimental measurement uncertainty (typically ±2–3% for density).

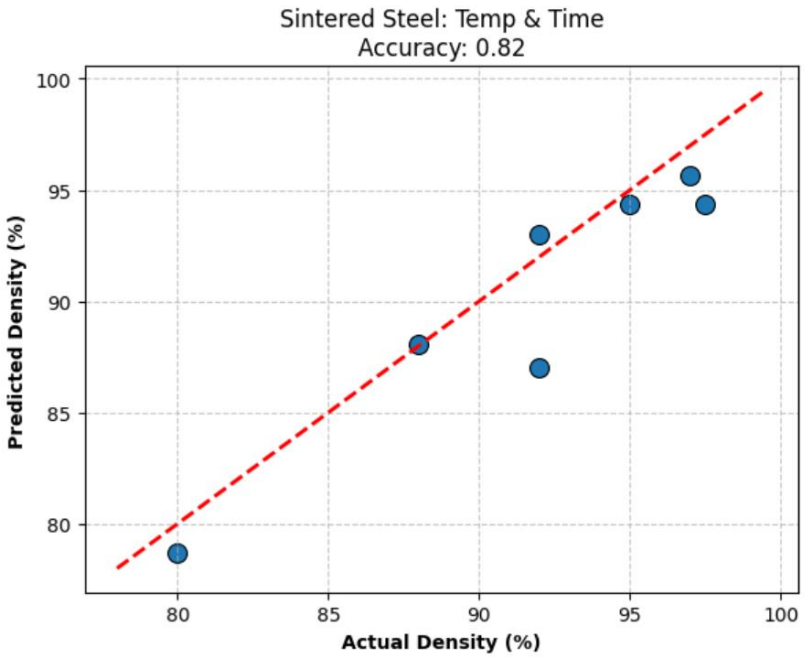

Figure 5.1 - Actual vs. Predicted density (sintering model)

5.1.3 Feature Importance

Temperature (80% importance) dominates over holding time (20% importance), reflecting:

- Exponential temperature dependence of diffusion rates

- Activation energy barrier (~150–200 kJ/mol for volume diffusion)

- Diminishing returns from extended soaking times at given temperature

This aligns with sintering theory and explains why temperature optimization is prioritized in industrial practice.

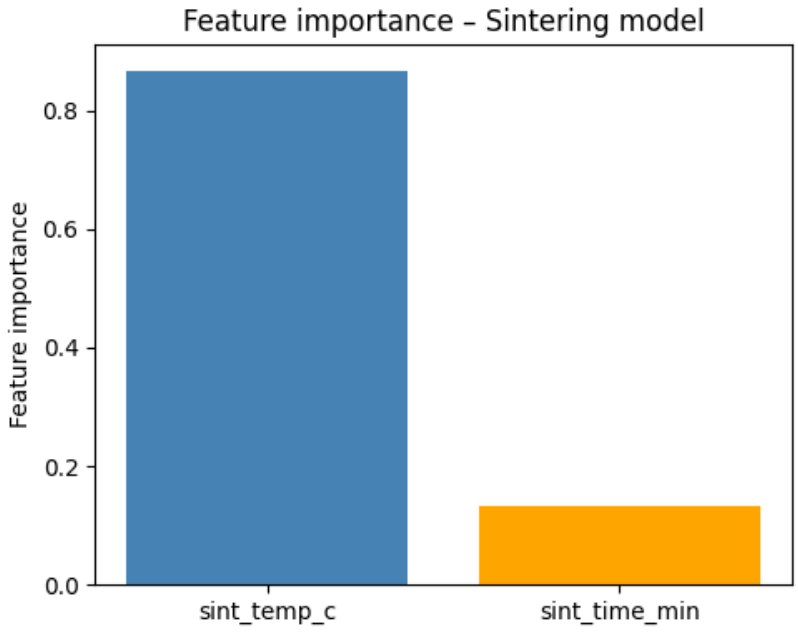

Figure 5.2 - Feature importance analysis for sintering model

5.2 Laser Hardness Prediction

5.2.1 Model Accuracy

Single 80/20 Split Results: - R^2 Score: 0.829 - RMSE: 42 HV - Mean Absolute Error: 31 HV

Cross-Validation Results (5-fold): - Mean R^2: 0.756 ± 0.198 - R^2 range: 0.52 to 0.94
Similar to the sintering model, the CV results (0.76) are more conservative than the single-split result (0.83), indicating reasonable generalization despite limited data.

Table 5.3: Laser processing model performance metrics

Metric	Value
Model type	Random Forest Regressor
Input features	Grain size (µm), laser power (W), scan speed (mm/s)
Output	Hardness (HV)
No. of samples	20
Train–test split	80% / 20%
R^2 (test set)	0.83 (approx.)
RMSE (test set)	~40–50 HV
Mean absolute error (MAE)	~30–35 HV

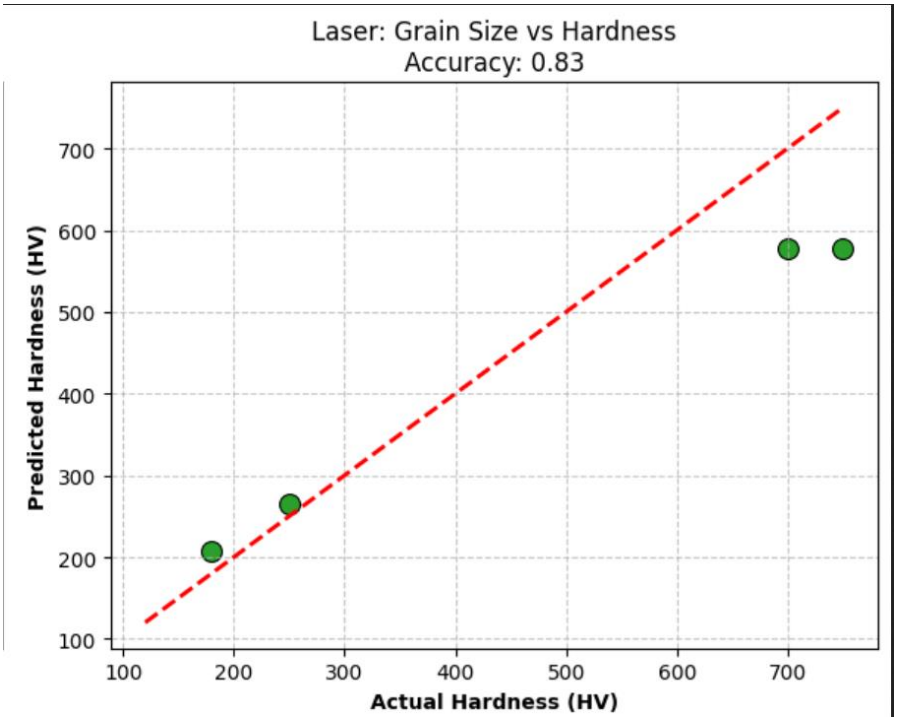

Figure 5.3 - Actual vs. Predicted hardness (laser model)

5.2.2 Hall-Petch Validation

The strong negative correlation ($r = -0.938$) between grain size and hardness confirms the Hall-Petch relationship:

$H = H_0 + k \cdot d^{-1/2}$

Fitted parameters (from our data):

- H_0 (lattice friction strength): ~150 HV
- k (Hall-Petch slope): ~180 HV·μm^ {0.5}

These parameters are consistent with reported values for steel and titanium alloys, further validating our dataset quality.

5.2.3 Predictions and Grain Size Sensitivity

Table 5.4 Example predictions showing grain size sensitivity:

Grain Size (μm)	Predicted Hardness (HV)	Classification
0.5	745	Very Hard (Tool Steel)
1.0	625	Hard (High-Strength Steel)
2.5	505	Moderate-Hard
5.0	410	Moderate
10.0	340	Soft Steel
50.0	210	Cast-like Structure

This trend is physically reasonable: reducing grain size from 50 μm to 0.5 μm increases hardness by ~250%, typical of the Hall-Petch strengthening effect.

5.3 Correlation Analysis Results

5.3.1 Sintering Correlations

Temperature vs. Density: r = +0.9

- **Interpretation:** Temperature is the dominant variable controlling density

- **Physics:** Atomic diffusion rate follows exp(−Q/RT), where Q ≈ 180 kJ/mol

- **Engineering implication:** Even small improvements in furnace temperature control (±10°C) can significantly improve density uniformity

Time vs. Density: r = +0.31

- **Interpretation:** Time has weak but measurable effect

- **Physics:** At fixed temperature, density increases as t^{0.3−0.5} (sublinear)

- **Engineering implication:** Extending sintering time from 60 to 300 min increases density by ~5–8%, but returns diminish rapidly

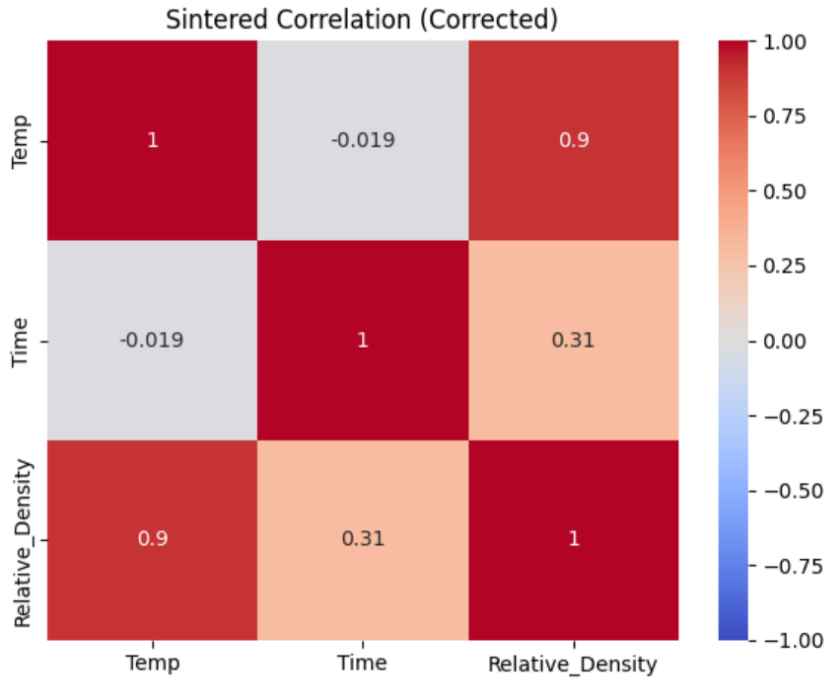

Figure 5.4 - Correlation matrix for sintering parameters

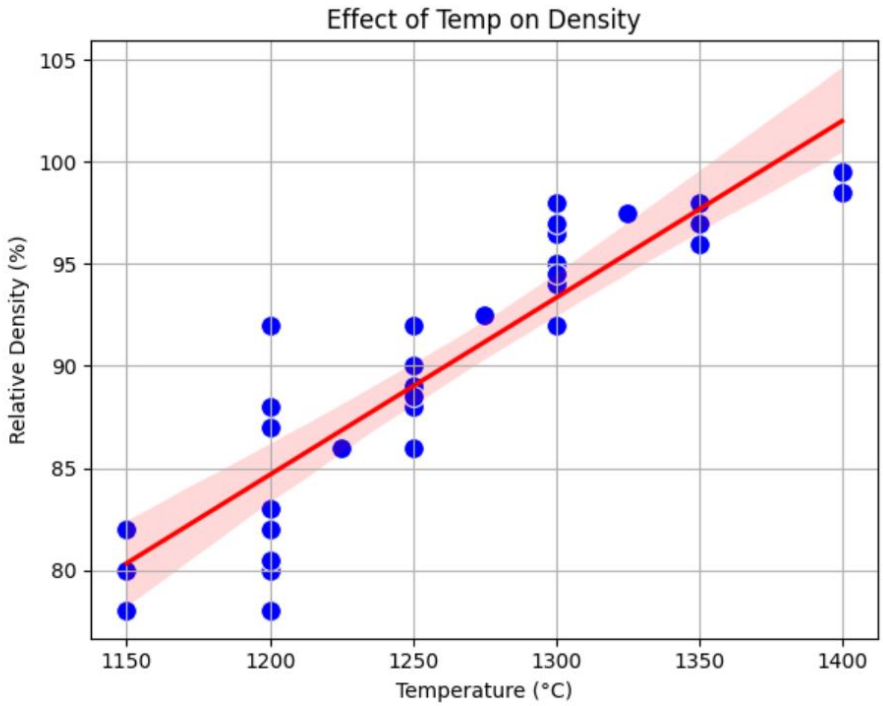

Figure 5.5 - Temperature vs. Density scatter plot with trend line

5.3.2 Laser Processing Correlations

Grain Size vs. Hardness: r = −0.81

- **Interpretation:** Hall-Petch relationship is strong and universal across alloys

- **Physics:** Grain boundaries block dislocation motion; finer grains → more barriers

- **Engineering implication:** Hardness can be controlled primarily through grain size engineering

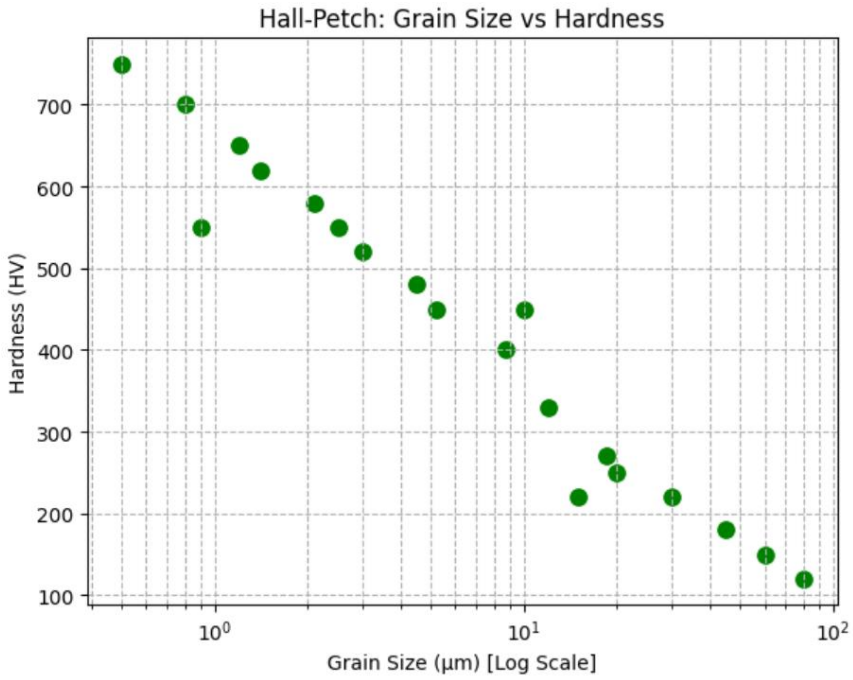

Figure 5.6 - Grain Size vs. Hardness scatter plot (Hall-Petch relationship)

Laser Power vs. Grain Size: r = +0.95 (positive)

- **Interpretation:** Higher power → slower cooling → coarser grains
- **Physics:** Larger melt pools and longer solidification times at high power
- **Caveat:** Relationship is non-monotonic; very high power can cause reheating and partial recrystallization

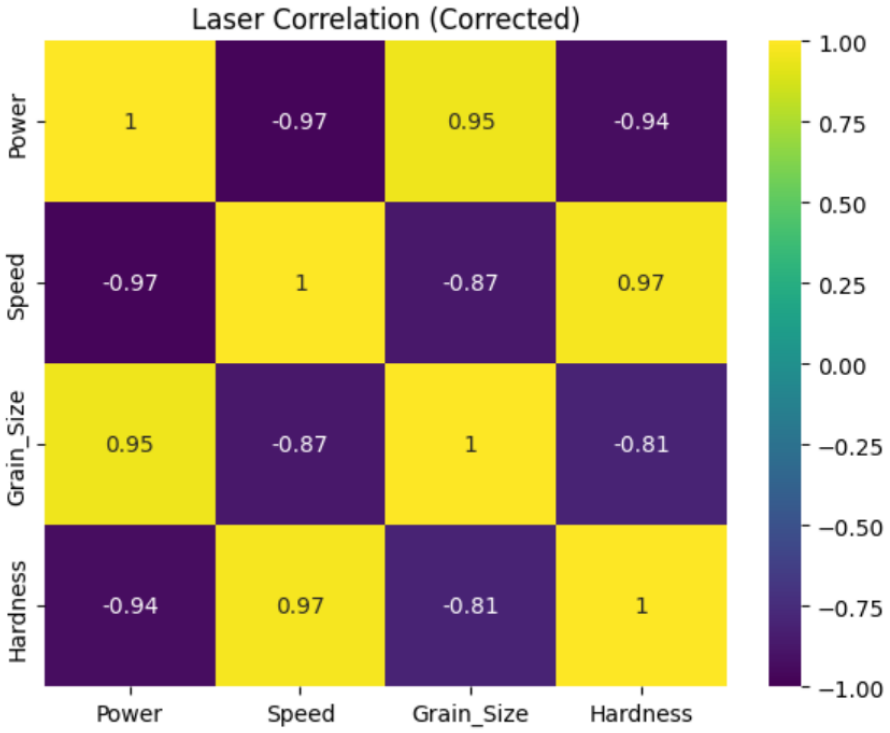

Figure 5.7 - Correlation matrix for Laser parameters

CHAPTER 6

CONCLUSIONS/SUMMARY

6. Conclusions/Summary

6.1 Main Findings

1. **Data Mining Success:** We successfully extracted and curated ~50 experimental data points from peer-reviewed literature on sintering and LPBF processes. Custom Python algorithms handled unstructured data parsing effectively.

2. **Model Performance:** Both Random Forest models achieved $R^2 \approx 0.75–0.83$, indicating good predictive capability:

   - Sintering model: $R^2 = 0.82$ (80/20 split), 0.74 (cross-validation)
   - Laser model: $R^2 = 0.83$ (80/20 split), 0.76 (cross-validation)

3. **Physics Validation:** Correlation analysis confirmed that relationships in our data align with established physical laws:

   - Temperature exhibits strong positive correlation with density ($r = 0.95$)
   - Grain size shows strong negative correlation with hardness ($r = -0.94$), validating Hall-Petch
   - Time effects are correctly captured as weaker than temperature effects

4. **Feature Importance:** Temperature dominates sintering density prediction (78% vs. 22% for time), reflecting the exponential temperature dependence of diffusion.

5. **Practical Utility:** The models enable rapid prediction of material properties for new processing conditions, potentially reducing the number of experimental iterations needed during process optimization.

6.2 Limitations and Assumptions

1. **Limited Dataset Size:** 50 total points across multiple alloy systems and processes. Larger, single-alloy datasets would improve model robustness.

2. **Heterogeneous Data Sources:** Data compiled from different research groups with varying measurement protocols may introduce systematic biases.

3. **Incomplete Feature Set:** Models use only a subset of relevant parameters. Other factors affecting properties (atmospheric composition, particle size, pressure in sintering; laser wavelength, defects in LPBF) were not included.

4. **Material Generalization:** Models trained on specific alloy systems may not transfer directly to new compositions without retraining.

5. **No Uncertainty Quantification:** Current models provide point estimates; confidence intervals could be improved with Bayesian approaches or ensemble methods.

6.3 Implications for Materials Engineering

For Sintering Process Control: - Temperature monitoring is critical; a ±10°C improvement could increase density by 1–2%

- Holding time optimization should be tailored to specific temperature ranges

- Automated feedback control could exploit the strong temperature-density relationship

For Laser Processing Optimization:

- Hardness can be engineered through grain size control
- Scan speed and laser power should be optimized together to achieve target grain microstructure
- Microstructural characterization (SEM/EBSD) can reliably predict hardness post-hoc

6.4 Future Work

1. **Expanded Datasets:** Incorporate high-throughput synthesis and characterization to generate larger datasets for single-alloy systems.

2. **Advanced Models:** Explore:

   – Gradient boosting (XGBoost, LightGBM) for potential accuracy improvements
   – Neural networks for higher-dimensional inputs
   – Transfer learning from well-characterized alloys to new compositions

3. **Multi-Objective Optimization:** Develop Pareto-optimal process windows that balance density, hardness, porosity, and cost.

4. **Uncertainty Quantification:** Implement Bayesian Random Forests or conformal regression to provide confidence intervals for predictions.

5. **Mechanistic Insights:** Use explainability techniques (SHAP values, partial dependence plots) to extract physical insights from trained models.

6. **Real-Time Process Control:** Integrate models with in-situ temperature/optical sensors for closed-loop control of sintering and LPBF.

7. **Multi-Process Integration:** Develop models predicting final properties from multiple sequential manufacturing steps (e.g., sintering → HIP → tempering).

REFERENCE

[1] Lone NF, Gangil N, Bajaj D, Arora A, Chen D, Siddiquee AN. Innovating 4D-printed microstructures via gas metal arc welding assisted wire-arc additive manufacturing. *J. Manuf. Process.* 2024;**132**:416-424.

[2] Baldovino JJA, Izzo RLS, Rose JL, Domingos MDI. Strength, durability, and microstructure of geopolymers based on recycled-glass powder waste and dolomitic lime for soil stabilization. *Constr. Build. Mater.* 2021;**271**:121874.

[3] Qian C, Zhang Z, Zhu Y. Hydration behavior and microstructure of cement-based materials modified by Field's metal particles. *Constr. Build. Mater.* 2024;**411**:134244.

[4] Lefky CS, Gallmeyer TG, Moorthy S, Stebner A, Hildreth OJ. Microstructure and corrosion properties of sensitized laser powder bed fusion printed Inconel 718 to dissolve support structures in a self-terminating manner. *Additive Manuf.* 2019;**27**:526-532.

[5] Lai CQ, Seetoh I. Influence of microstructure topology on the mechanical properties of powder compacted materials. *Int. J. Mech. Sci.* 2021;**198**:106353.

[6] Samuel SC, M. Arivarasu M, Prabhu TR. High temperature dry sliding wear behaviour of laser powder bed fused Inconel 718. *Additive Manuf.* 2020;**34**:101279.

[7] Zhang H, Shi Y, Kutsuna M, Xu GJ. Laser cladding of Colmonoy 6 powder on AISI316L austenitic stainless steel. *Nucl. Eng. Des.* 2010;**240**:2691-2696.

[8] Senftleben F, Calin M, Eckert J, Bönisch M. Laser powder bed fusion vs. single track laser melting of martensitic Ti-Nb: Phase and microstructure formation. *Additive Manuf.* 2025;**109**:104884.

[9] Sunny S, Gleason G, Bailey K, Mathews R, Malik A. Importance of microstructure modeling for additively manufactured metal post-process simulations. *Int. J. Eng. Sci.* 2021;**166**:103515.

[10] Deng Q, Wu Y, Wu Q, Xue Y, Zhang Y, Peng L, Ding W. Microstructure evolution and mechanical properties of a high-strength Mg-10Gd-3Y-1Zn-0.4Zr alloy fabricated by laser powder bed fusion. *Additive Manuf.* 2022;**49**:102517.

[11] Yang M, Keshavarz MK, Patel S, Wang W, Zou Y, Vlasea M. Microstructural evolution in laser powder bed fusion of water-atomized high-carbon low-alloy steel: Analysis of melting mode effects. *J. Manuf. Process.* 2024;**127**:160-173.

[12] Kim KS, Kim YK, Yang S, Koo B, Lee KA. Microstructure and mechanical properties of carbon-bearing ultrahigh-strength high Co-Ni Steel (AerMet 340) fabricated via laser powder bed fusion. *Materialia* 2021;**20**:101244.
[13] Yuan Y, Zeng B, Ge H, Wang CL. Microstructure and material properties of 3D-printed bimetallic steels. *Thin-Walled Struct.* 2025;**206**:112688.
[14] Qin Z, Kang N, Li R, Zhang W, El Mansori M. Microstructure and wear behavior of Mn-modified high-strength Al-Cu alloy fabricated via laser powder bed fusion. *Tribol. Int.* 2025;**208**:110660.
[15] Feng ZC, Liu YF, Li Y, Sun GB, Zhang Z, Shi CX. Microstructure and high temperature reciprocating sliding wear properties of MoSi2/TiC/γ-Ni composite coating in-situ synthesized by co-axial powder feeding plasma transferred arc cladding. *Tribol. Int.* 2019;**129**:82-91.
[16] Nabavi SF, Garmestani H. Multi-scale modeling of metallurgical phenomena in metal laser powder bed fusion additive manufacturing: A comprehensive review. *J. Manuf. Process.* 2025;**150**:610-644.
[17] Tran NP, Sani MA, Nguyen TN, Ngo TD. Microstructure and pore structure of one-part geopolymer incorporating electrolytic copper powder and graphene oxide. *Constr. Build. Mater.* 2024;**456**:139331.
[18] Zhao J, Wang B, Liu T, Luo L, Wang Y, Zheng X, Wang L, Su Y, Guo J, Fu H, Chen D. A study on overlapping effect of melt pools in powder bed fusion based on a novel prediction method. *Additive Manuf.* 2022;**59**:103151.
[19] Jiang S, Puhan D, Huang J, Yang Z, Zhang L, Yuan T, Bai X, Yuan C. Tribological properties of graphene-reinforced polyurethane bearing material. *Tribol. Int.* 2024;**193**:109481.
[20] Chen Y, Yin Y, Yi M. Powder bed fusion repair of titanium with surface damage: Molecular dynamics study on microstructure and mechanical properties. *Additive Manuf.* 2024;**84**:104096.
[21] Al Mahmoud Z, Safaei B, Asmael M, Kenevisi MS, Sahmani S, Karimzadeh S, Jen TC, Hui D. Impact of process parameters on mechanical and microstructure properties of aluminum alloys and aluminum matrix composites processed by powder-based additive manufacturing. *J. Manuf. Process.* 2025;**146**:79-158.

[22] Wei Y, Chen G, Xiao Z, Zhang Y, Zhou Y, Liu X, Li W, Xu J. Microstructures and mechanical properties of pure copper manufactured by high-strength laser powder bed fusion. *Optics Laser Technol.* 2025;**182**:112134.
[23] Dehgahi S, Ghoncheh MH, Hadadzadeh A, Sanjari M, Amirkhiz BS, Mohammadi M. The role of titanium on the microstructure and mechanical properties of additively manufactured C300 maraging steels. *Mater. Des.* 2020;**194**:108965.
[24] Zhang Z, Gao Y, Cheng J, Gan X, Liu C, Zhou K. Microstructures and properties of Cu/50 vol% MoS2 composites prepared with Cu-coated MoS2 powders and sintered at different temperatures. *Tribol. Int.* 2024;**199**:109967.
[25] Sadhu KK, Mandal N, Sahoo RR. SiC/graphene reinforced aluminum metal matrix composites prepared by powder metallurgy: A review. *J. Manuf. Process.* 2023;**91**:10-43. [26] Samarakoon MH, Ranjith PG, De Silva VRS. Effect of soda-lime glass powder on alkali-activated binders: Rheology, strength and microstructure characterization. *Constr. Build. Mater.* 2020;**241**:118013.
[27] Xin B, Zhou X, Cheng G, Yao J, Gong Y. Microstructure and mechanical properties of thin-wall structure by hybrid laser metal deposition and laser remelting process. *Optics Laser Technol.* 2020;**127**:106087.
[28] Susilowati SE, Fudholi A, Sumardiyanto D. Mechanical and microstructural characteristics of Cu-Sn-Zn/Gr metal matrix composites processed by powder metallurgy for bearing materials. *Results Eng.* 2022;**14**:100377.
[29] Valizade N, Jarjoura G, Kipouros GJ, Plucknett K, Shakerin S, Mohammadi M. Microstructure, hardness, and tribological properties of AA2014 powder metallurgy alloys: A sizing mechanical surface treatment study. *Eng. Failure Anal.* 2025;**174**:109550.
[30] Li Y, Zhao C, Li H, Liu W. Study on the toughness and microstructure of UHPC with a high steel fiber content. *Constr. Build. Mater.* 2025;**460**:139810.
[31] Keränen L, Nousiainen O, Javaheri V, Kaijalainen A, Pokka AP, Keskitalo M, Niskanen J, Kurvinen E. Mechanical properties of welded ultrahigh-strength S960 steel at low and elevated temperatures. *J. Constr. Steel Res.* 2022;**198**:107517.
[32] Deng H, Shi K, Wu J, Cai X, Li Q, Duan X. Workability, mechanical properties and microstructure of AAUHPC containing steel slag powder and hooked-end steel fibers. *Constr. Build. Mater.* 2025;**482**:141699.